J|A|C|S
ARTICLES
Published on Web 05/09/2002

Quenching of Tryptophan $^1(\pi,\pi^*)$ Fluorescence Induced by Intramolecular Hydrogen Abstraction via an Aborted Decarboxylation Mechanism

Lluís Blancafort,[†,§] David González,[†] Massimo Olivucci,[‡] and Michael A. Robb*[,†]

Contribution from the Department of Chemistry, King's College London, Strand, London WC2R 2LS, U.K., and Dip. di Chimica, Università degli Studi di Siena, Via Aldo Moro, I-53100 Siena, Italy

Received August 22, 2001

Abstract: CASSCF computations show that the hydrogen-transfer-induced fluorescence quenching of the $^1(\pi,\pi^*)$ excited state of zwitterionic tryptophan occurs in three steps: (1) formation of an intramolecular excited-state complex, (2) hydrogen transfer from the amino acid side chain to the indole chromophore, and (3) radiationless decay through a conical intersection, where the reaction path bifurcates to a photodecarboxylation and a phototautomerization route. We present a general model for fluorescence quenching by hydrogen donors, where the radiationless decay occurs at a conical intersection (real state crossing). At the intersection, the reaction responsible for the quenching is aborted, because the reaction path bifurcates and can proceed forward to the products or backward to the reactants. The position of the intersection along the quenching coordinate depends on the nature of the states and, in turn, affects the formation of photoproducts during the quenching. For a $^1(n,\pi^*)$ model system reported earlier (Sinicropi, A.; Pogni, R.; Basosi, R.; Robb, M. A.; Gramlich, G.; Nau, W. M.; Olivucci, M. *Angew. Chem., Int. Ed.* **2001**, *40*, 4185−4189), the ground and the excited state of the chromophore are hydrogen acceptors, and the excited-state hydrogen transfer is nonadiabatic and leads directly to the intersection point. There, the hydrogen transfer is aborted, and the reaction can return to the reactant pair or proceed further to the hydrogen-transfer products. In the tryptophan case, the ground state is not a hydrogen acceptor, and the excited-state hydrogen transfer is an adiabatic, sequential proton and electron transfer. The decay to the ground state occurs along a second reaction coordinate associated with decarboxylation of the amino acid side chain and the corresponding aborted conical intersection. The results show that, for $^1(\pi,\pi^*)$ states, the hydrogen transfer alone is not sufficient to induce the quenching, and explain why fluorescence quenching induced by hydrogen donors is less general for $^1(\pi,\pi^*)$ than for $^1(n,\pi^*)$ states.

Introduction

In recent years, theoretical chemistry has shown the crucial role of conical intersections (real state crossings) in the radiationless decay of electronically excited states.[1] The conical intersection points provide an efficient decay funnel from the excited to the ground state for barrierless, ultrafast processes[2] and for thermally activated processes associated with longer lifetimes. Computational studies have shown that such a mechanism is involved in hydrogen-transfer processes in the excited state, which are associated with quenching of the fluorescence (radiationless decay).[3] For instance, the quenching of the n,π^* singlet excited state of a model azoalkane by a hydrogen donor (dichloromethane) takes place via a conical intersection.[3a,b] At the intersection, the reaction path is bifurcated towards the original reactant pair (aborting the process), or the hydrogen-transfer products. In a similar manner, the intramolecular quenching of a benzotriazole analogue, a model for photostabilizing industrial additives, also goes through a conical intersection.[3c] In this paper, we turn our attention to the intramolecular fluorescence quenching of the singlet π,π^* state of zwitterionic tryptophan (TRP).[4] Our CASSCF/6-31g* results show that the radiationless decay takes place in three steps with low energy barriers, as shown in Figure 1: (1) formation of an excited-state complex **S_1-Exc** on the excited S_1 potential energy

* To whom correspondence should be addressed. E-mail: mike.robb@kcl.ac.uk.
† King's College London.
‡ Università degli Studi di Siena.
§ Current address: Institut de Química Computacional, Universitat de Girona, E-17071 Girona, Spain.

(1) (a) Robb, M. A.; Garavelli, M.; Olivucci, M.; Bernardi, F. In *Reviews in Computational Chemistry*; Lipkowitz, K. B., Boyd, D. B., Eds.: Wiley-VCH: New York, 2000; Vol. 15, pp 87−212. (b) Bernardi, F.; Olivucci, M.; Robb, M. A. *Chem. Soc. Rev.* **1996**, *25*, 321−328. (c) Klessinger, M.; Michl, J. *Excited States and Photochemistry of Organic Molecules*; VCH: New York, 1995; pp 182−186.
(2) (a) Sánchez-Gálvez, A.; Hunt, P.; Robb, M. A.; Olivucci, M.; Vreven, T.; Schlegel, H. B. *J. Am. Chem. Soc.* **2000**, *122*, 2911−2924. (b) Garavelli, M.; Celani, P.; Bernardi, F.; Robb, M. A.; Olivucci, M. *J. Am. Chem. Soc.* **1997**, *119*, 11487−11494.
(3) (a) Sinicropi, A.; Pogni, R.; Basosi, R.; Robb, M. A.; Gramlich, G.; Nau, W. M.; Olivucci, M. *Angew. Chem., Int. Ed.* **2001**, *40*, 4185−4189. (b) Nau, W. M.; Greiner, G. H.; Wall, J.; Rau, H.; Olivucci, M.; Robb, M. A. *Angew. Chem., Int. Ed.* **1998**, *37*, 98−101. (c) Estévez, C. M.; Bach, R. D.; Hass, K. C.; Schneider, W. F. *J. Am. Chem. Soc.* **1997**, *119*, 5445−5446.
(4) (a) Eftink, M. In *Methods of Biochemical Analysis. Volume 35: Protein Structure Determination*; Suelter, C. H., Ed.; John Wiley & Sons: New York, 1991; Vol. 35, pp 127−203. (b) Creed, D. *Photochem. Photobiol.* **1984**, *39*, 537−562.

10.1021/ja016915a CCC: $22.00

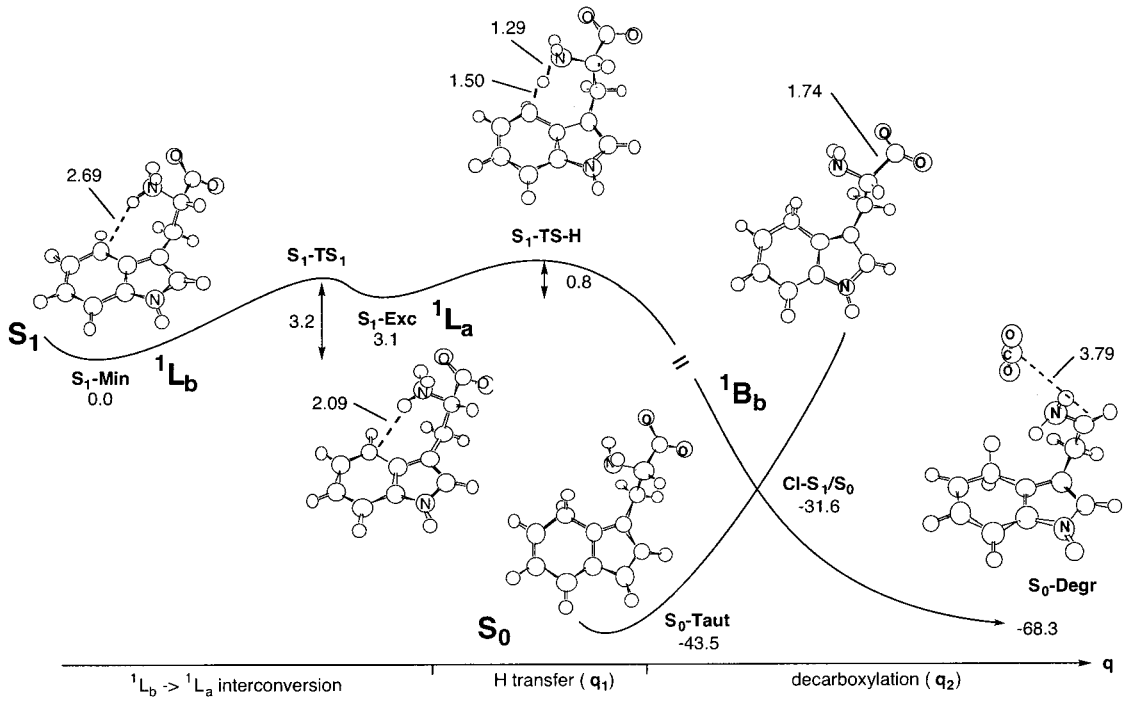

Figure 1. Reaction coordinate and energetics for TRP fluorescence quenching induced by hydrogen transfer and aborted decarboxylation.

surface, preceded by interconversion of two low-lying excited states (a covalent and an ionic one, denoted ^1L_b and ^1L_a in Platt's nomenclature[5]); (2) hydrogen transfer from the side chain to the chromophore (tautomerization) in the excited state; and (3) radiationless decay through a conical intersection, **CI-S_1/S_0**. In contrast to the azoalkane case, the radiationless decay occurs after the hydrogen transfer is complete on S_1, and is associated with decarboxylation of the side chain.

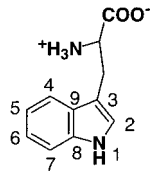

The difference between the aborted hydrogen-transfer mechanism found for the n,π^* azoalkane model and the quenching through complete tautomerization and decarboxylation, described here for TRP (π,π^* case), can be explained in terms of two related factors: (1) the position of the crossing point (conical intersection) along the relaxation coordinate (*nuclear* or *geometric* factor) and (2) the correlation between two diabatic states for the hydrogen transfer (*electronic* factor). The geometric factor affects the product distribution, because the conical intersection acts as a bifurcation between two possible reaction products (see Figure 2). For the aborted type of surface (Figure 2a), found for the n,π^* azoalkane reaction, there is an early state crossing along the primary photochemical reaction coordinate.[3a,b] After the crossing, the reaction can proceed forward to the product **P** or backward to the reactant **R**. In the alternative situation, described here for TRP, the conical intersection occurs after the primary reaction is complete. In this case (Figure 2b), a primary photoproduct **P*** is formed in the excited state, and the decay takes place along a different

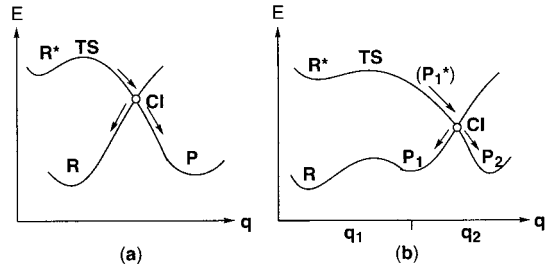

Figure 2. General potential energy surfaces for photochemistry (peaked conical intersection). (a) "Aborted" primary process. (b) "Completed" primary process.

coordinate $\mathbf{q_2}$, which, in turn, is aborted. Thus, the reaction path branches between two different products $\mathbf{P_1}$ and $\mathbf{P_2}$. In the TRP case, the two coordinates are hydrogen transfer ($\mathbf{q_1}$) and decarboxylation ($\mathbf{q_2}$).

The origin of the different surface topologies described above lies in the correlation between the two diabatic states for hydrogen transfer. The general correlation diagram, initially derived for hydrogen abstraction by n,π^* excited carbonyl compounds,[6] is shown in Scheme 1. The reactants are connected to the products *diabatically* by the dashed lines, and there are two reactant−product diabatic states. One connects closed-shell structures, and the diabatic reaction coordinate is a proton transfer. The other diabatic state connects open-shell structures, and the reaction involves hydrogen radical transfer. Thus, the hydrogen transfer can take place in two different ways. When the reaction starts on the upper state (open-shell reactants), the formation of the lower state products (path a) is nonadiabatic and goes through a conical intersection (a crossing with the closed-shell pair state). On the other hand, the lower state reaction is adiabatic (path b), and the hydrogen transfer takes

(5) Platt, J. R. *J. Chem. Phys.* **1949**, *17*, 489.

(6) Turro, N. J. *Modern Molecular Photochemistry*; University Science Books: Sausalito, CA, 1991; pp 219−224. (b) Salem, L. *Electrons in Chemical Reactions: First Principles*; John Wiley & Sons: New York, 1982; pp 135−139.

Scheme 1

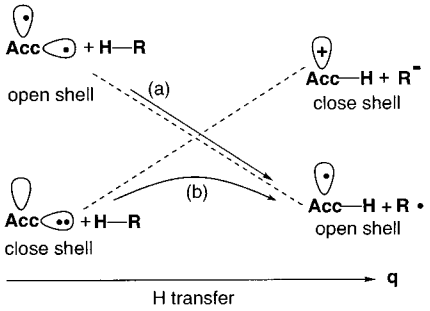

place along an avoided crossing path through a transition structure.

In this context, to clarify the terms *diabatic* and *nonadiabatic*, we stress that the diabatic states (dashed lines of the correlation diagram) have not been calculated but are only an "idealized" representation of the "pure" proton and hydrogen radical transfer processes. The full lines of Scheme 1 represent the adiabatic surfaces obtained from our ab initio calculations. Path a is nonadiabatic because a real surface crossing is involved, while path b is adiabatic because it takes place only on one potential energy surface along an avoided crossing. Moreover, the real crossing and the avoided crossing (and, therefore, paths a and b) can coexist on the same multidimensional potential energy surface, along different geometric coordinates.[1,7] In this case, the surface of the lower state, near the intersection, has the shape of a moat, and the adiabatic path lies on the moat. We have previously described such surfaces in detail for ground-state electron-transfer reactions,[8] and a similar surface has been found for the azoalkane model calculations discussed here.[3a,b]

The two quenching processes can now be discussed using the concepts introduced above. The different surface topologies found for the n,π^* and the π,π^* case arise from the different role of the ground state of the acceptor. In the azoalkane n,π^* model (Figure 3a), the ground state is a proton acceptor because of the nitrogen lone pair. Thus, the two correlated diabatic states in the general diagram of Scheme 1 correspond to the ground and the excited state. The reaction starts in the upper state and follows the nonadiabatic path a (Scheme 1), going through the conical intersection. The topology corresponds to the aborted reaction coordinate (Figure 2a), and mechanistically the reaction is a pure hydrogen radical transfer. In contrast to this, the ground state of the TRP chromophore is a delocalized, aromatic species which is not a good hydrogen acceptor. Thus, the two correlated states are the two excited states of the indole chromophore shown in Figure 3b (reactant side), the ionic ^1L_a and a biradical ^1B_b state. Therefore, the hydrogen transfer follows an excited-state adiabatic path b (Scheme 1). It starts on the lower state of the general correlation diagram (S_1 on the potential energy surface) and leads to the open-shell tautomer **S_1-Taut** shown in Figure 3b. Mechanistically, the reaction coordinate for TRP starts as a proton transfer, but due to the mixing of the states along the avoided crossing it results in a net hydrogen radical transfer. Our calculations show that the mixing of the ionic and biradical states only starts when the proton transfer is almost

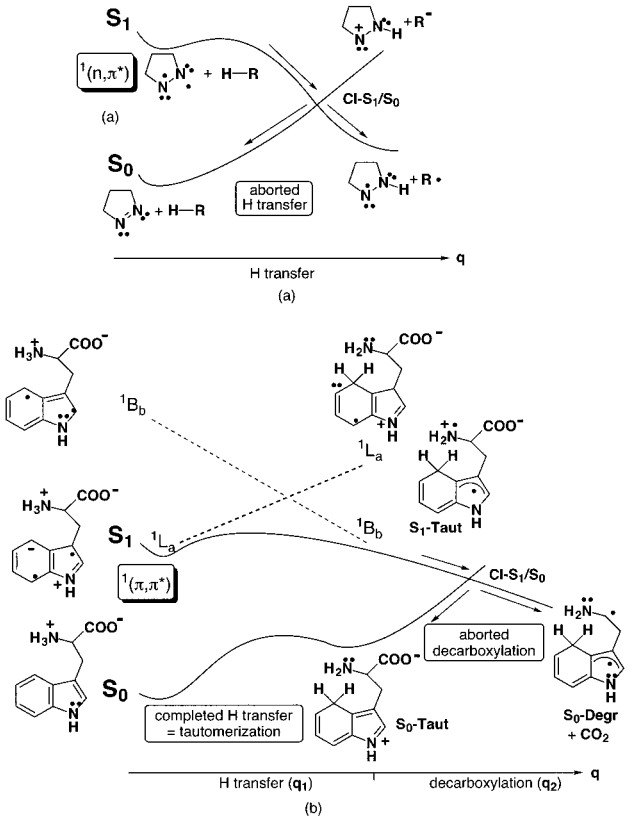

Figure 3. Reaction coordinates for fluorescence quenching induced by excited-state hydrogen abstraction. (a) $^1(n,\pi^*)$ case (R=$CHCl_2$), aborted H-transfer intersection. (b) $^1(\pi,\pi^*)$ case, completed H transfer with aborted decarboxylation intersection.

complete. It is, therefore, equivalent to an electron transfer from the side chain (primarily the amino group) to the chromophore. Therefore, the mechanism of the π,π^* abstraction is best described as a coupled, sequential proton and electron transfer.

The charge generated in the amine group (see structure **S_1-Taut** of Figure 3b) is delocalized along the nitrogen and oxygen lone pairs and the σ carbon−carbon bond of the side chain. However, the excited-state tautomer is not a stationary point on the potential energy surface because the carbon−carbon cleavage through the intersection **CI-S_1/S_0** is barrierless. At the intersection, the reaction path bifurcates toward two products (Figure 1): the ground-state tautomer **S_0-Taut** and the degradation product **S_0-Degr**, precursor of the photodecarboxylation product tryptamine. Therefore, the second part of the quenching coordinate for TRP follows an "aborted decarboxylation mechanism".

Our results suggest that intermolecular (azoalkane model)[3a,b] or intramolecular (TRP) aborted photochemical reactions may well be general features of the radiationless deactivation mechanism in certain organic molecules. The aborted photochemical reaction follows the general mechanism outlined in Scheme 2 for TRP. Thus, the reaction can decay at either of two sides of the intersection. One branch leads to a radical pair (a ground-state intermediate, **S_0-Degr**), whereas the opposite branch leads to an ion pair. However, the ion pair is unstable, and the second branch ends in regeneration of the reactant (the nondecarboxylated **S_0-Taut**), so that the reaction is aborted along that branch. From the electronic point of view, the two ground-state ion and radical pairs are connected by an *intra*molecular electron transfer between the side chain and the protonated

(7) (a) Davidson, E. R. *J. Am. Chem. Soc.* **1977**, *99*, 397−402. (b) Herzberg, G. *Electronic Spectra of Polyatomic Molecules*; Van Nostrand: New York, 1966; pp 48, 449.
(8) Blancafort, L.; Jolibois, F.; Olivucci, M.; Robb, M. A. *J. Am. Chem. Soc.* **2001**, *123*, 722−732.

Scheme 2

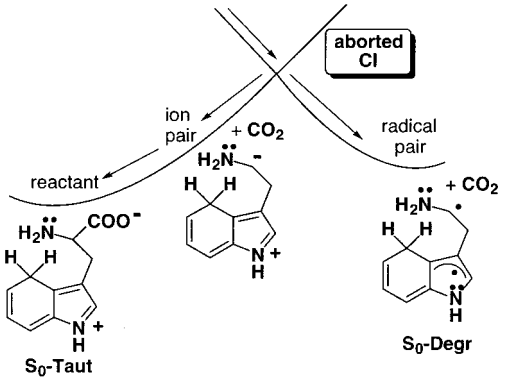

chromophore. The same situation has been described for the aborted hydrogen transfer in the azoalkane case, although there the ion and radical pairs are related by an *inter*molecular electron transfer.[3a] Therefore, the ground-state decarboxylation path of TRP (from **S_0-Taut** to **S_0-Degr**), and the ground-state hydrogen transfer of the azoalkane and dichloromethane model system, are *adiabatic sequential bond cleavage and electron-transfer reactions*. As shown for the azoalkane case,[3a] the conical intersection point lies very close to the transition structure for the ground-state reaction, which makes clear why the radiationless decay path bifurcates to reactants or products.

From the point of view of the photophysics and photochemistry of TRP, our calculations clarify the mechanism of the fluorescence quenching found in TRP at neutral and slightly acidic pH.[4,9,10] This is one of several intriguing properties of TRP photophysics, which include the interconversion of the ^1L_a and ^1L_b states at the picosecond scale,[9a] the solvent dependence (large Stokes shift in water), and the doubly exponential fluorescence decay at the nanosecond scale. Experimentally, the fluorescence lifetime in water decreases when going from basic (pH $\approx$ 11, $\tau \approx 9$ ns) to neutral and acidic (pH $\leq$ 7, $\tau \approx 3$ ns) conditions at room temperature, and a second, short-lived component ($\tau \approx 0.4$ ns) appears. The key role of the intramolecular hydrogen transfer in the quenching was proved by experiments in deuterated solvents, which resulted in deuterium incorporation at the C_4 position of the indole chromophore, and by the recovery of the fluorescence by complexation of the protonated side chain with a crown ether.[10] The short-lived fluorescence component at pH $\leq$ 7 is attributed to one of six possible side-chain conformers,[9b,c,f] where the protonated amino function is oriented correctly for the hydrogen transfer that induces the quenching. In the remaining conformers, the amino group is turned away from the chromophore, and the fluorescence should not be effected by the pH. With our calculations we have investigated the quenching mechanism for the zwitterionic form of tryptophan, which will be dominant near its isoelectric point (pH 5.89). Different mechanisms may be involved at other pH values or in the gas phase. Our computations reveal that the hydrogen transfer is intimately related to the photodecarboxylation of the molecule.[11] In fact, the two reactions are associated with a *single transition structure*, and the reaction paths *bifurcate at a conical intersection*. As a consequence, the reactions cannot be analyzed by classic transition state theory because one of its central assumptions, the reversibility of the reaction, no longer holds.[12] This is a general characteristic of reactions that go through bifurcations, and in this respect the conical intersection can be seen as the excited-state equivalent of a ground-state bifurcation associated with a valley ridge inflection point.[13,14]

Moreover, our calculations also explain why the quenching of singlet π,π^* states by hydrogen (or proton) donors[10,15] is not as general as for n,π^* states.[16] In fact, intramolecular proton-induced fluorescence quenching has been also observed in tryptamine[10a] and in aminoalkylated naphthalenes[15a] and benzenes.[15c] However, the fluorescence of the parent indole[4] and naphthalene[15b] molecules is constant at the pH range 3−11, and quenching by H_3O^+ has been only observed in donor-substituted naphthalenes.[15b] The reason is clearly that for π,π^* excited states, the hydrogen transfer alone is not sufficient to induce the crossing to the ground state, and an additional reaction (a bond cleavage) is necessary to reach the point of radiationless decay.

Computational Details

For our study of the proton-transfer-induced quenching, we have used the zwitterionic form of tryptophan, where the amino acid chain contains a protonated ammonium group and a carboxylate anion. We do not expect this isomer to be the lowest-energy one in the gas phase (it should be the one where the amino and acid functionalities remain neutral), but we chose the zwitterionic form, which is the most stable one in water near its isoelectronic point (pH 5.89), to model the reaction of interest in this solvent. The zwitterionic conformers of TRP are gas-phase minima at the HF/6-31G* level of theory, and for our study we started from the optimized ground-state conformer where the protonated ammonium is closest to the benzene moiety of the indole chromophore. This conformer is prearranged for the proton transfer to the ring.

For our ab initio calculations on the photophysics of tryptophan, we have used the CASSCF/6-31G* level of theory, with an active space of 10 electrons in nine orbitals (except where noted, see below). No Rydberg orbitals were included. The Cartesian coordinates of the

(9) (a) Ruggiero, A. J.; Todd, D. C.; Fleming, G. R. *J. Am. Chem. Soc.* **1990**, *112*, 1003−1014. (b) Philips, L. A.; Webb, S. P.; Martinez, S. J., III; Fleming, G. R.; Levy, D. H. *J. Am. Chem. Soc.* **1988**, *110*, 1352−1355. (c) Rizzo, T. R.; Park, Y. D.; Levy, D. H. *J. Chem. Phys.* **1986**, *85*, 6945−6951. (d) Gudgin-Templeton, E. F.; Ware, W. R. *J. Phys. Chem.* **1984**, *88*, 4626−4631. (e) Robbins, R. J.; Fleming, G. R.; Beddard, G. S.; Robinson, G. W.; Thistlethwaite, P. J.; Woolfe, G. J. *J. Am. Chem. Soc.* **1980**, *102*, 6271−6279. (f) Szabo, A. G.; Rayner, D. M. *J. Am. Chem. Soc.* **1980**, *102*, 554−563. (g) Bent, D. V.; Hayon, E. *J. Am. Chem. Soc.* **1975**, *97*, 2612−2619.

(10) (a) Shizuka, H.; Serizawa, M.; Shimo, T.; Saito, I.; Matsuura, T. *J. Am. Chem. Soc.* **1988**, *110*, 1930−1934. (b) Saito, I.; Sugiyama, H.; Yamamoto, A.; Muramatsu, S.; Matsuura, T. *J. Am. Chem. Soc.* **1984**, *106*, 4286−4287.

(11) (a) Roshchupkin, D. I.; Talitsky, V. V.; Pelenitsyn, A. B. *Photochem. Photobiol.* **1979**, *30*, 635−643. (b) Hasselmann, C.; Pigault, C.; Santus, R.; Laustriat, G. *Photochem. Photobiol.* **1978**, *27*, 13−18.

(12) Atkins, J. *Physical Chemistry*; Oxford University Press: Oxford, 1998; pp 830−834.

(13) (a) Bakken, V.; Danovich, D.; Shaik, S.; Schlegel, H. B. *J. Am. Chem. Soc.* **2001**, *123*, 130−134. (b) Schlegel, H. B. In *Encyclopedia of Computational Chemistry*; Schleyer, P.v. R., Allinger, N. L., Clark, T., Gasteiger, J., Kollman, P. A., Schaefer, H. F., III, Schreiner, P. R., Eds.; Wiley: Chichester, 1998; pp 2432−2437.

(14) Recently, one of us has shown that the situation can be more complicated and that there can be *three* available ground-state reaction channels starting from the tip of an intersection. See: Garavelli, M.; Bernardi, F.; Moliner, V.; Olivucci, M. *Angew. Chem., Int. Ed.* **2001**, *40*, 1466−1468.

(15) (a) Shizuka, H. *Acc. Chem. Res.* **1985**, *18*, 141−147. (b) Shizuka, H.; Tobita, S. *J. Am. Chem. Soc.* **1982**, *104*, 6919−6927. (c) Shizuka, H.; Nakamura, M.; Morita, T. *J. Phys. Chem.* **1979**, *83*, 2019−2024.

(16) We refer here to quenching processes where the hydrogen donor is not part of the chromophore. Other typical examples of excited-state intramolecular proton transfer associated with fluorescence quenching, where the hydrogen donor is part of the chromophore, such as hydroxyphenyl benzotriazoles, may not adjust to the model proposed here. For a recent review, see: Waluk, J. In *Conformational Analysis of Molecules in Excited States*; Waluk, J., Ed.; Wiley-VCH: New York, 2000; pp 57−112. See also ref 3c.

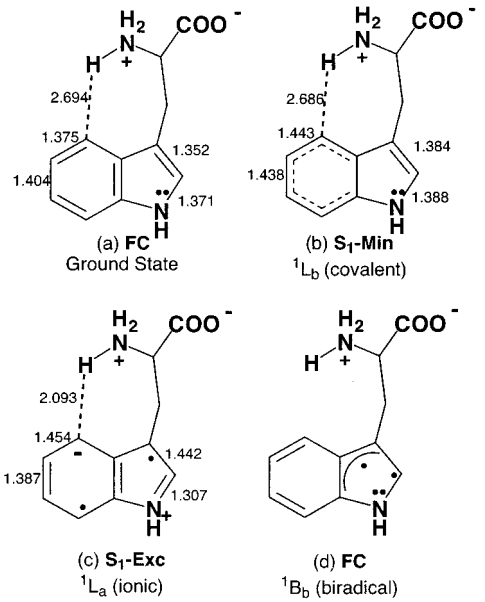

Figure 4. Optimized geometries (bond lengths in Å) and resonance structures for the ground state and the three excited states (covalent, ionic, and biradical) of TRP. Biradical state resonance structure refers to the Franck−Condon (FC) geometry.

optimized structures and the results of the analytical frequency calculations are given in the Supporting Information section. Stateaverage coefficients between S_1 and S_2 (0.5/0.5) and S_1, S_2, and S_3 (0.33/0.33/0.33) were used for the orbitals of the second and third excited state, respectively. All stationary points (minima, transition structures, and conical intersections) have been optimized with a development version of the Gaussian 98 package of programs.[17] Analytical frequency calculations with an (8,8) reduced active space were carried out for the optimized TS's. The energetics of the excited-state complex formation and the hydrogen transfer have been recomputed with CAS-MP2 single-point calculations using a new procedure based on localization of the active space orbitals.[18] The complete list of CASSCF and CAS-MP2 energies is given in Table S1, Supporting Information.

Results: Computation and Analysis of Critical Points on the Potential Energy Surface

Valence-Bond Analysis of the Structures. The wave functions of the optimized ground and excited-state structures were analyzed on the basis of a valence-bond derived model for which the orbitals of the active space are localized (see Figures 4 and 5).[19] The D_{ii} elements (diagonal elements of the one-electron density matrix of the active space, italic numbers in Figure 5) give the occupation numbers of the localized π orbitals (ideally, 1.0 for carbon and 2.0 for nitrogen neutral atoms), and the P_{ij} elements (spin-exchange density matrix elements, only $\alpha\beta$ components were considered) between neighboring atoms give an estimate of the π bond order (maximum value of 1.0). The calculated D_{ii} and P_{ij} values for the most relevant structures are shown in Figure 5, and a complete list is given in the Supporting Information section, Table S2.

The valence-bond structures derived by this analysis for the ground and the three lowest excited valence states, computed at the Franck−Condon (FC) geometry, are given in Figure 4 (together with the most important bond lengths of the optimized structures). The bonding in the ground state is best described by alternating single and double bonds (see Figure 4a). These bond orders (Figure 5a) are derived from a high P_{ij} element for the C_2-C_3 pyrrole double bond (0.48) and medium values in the benzene ring. The occupation of the localized nitrogen orbital is 1.69, showing partial delocalization of the nitrogen lone pair into the ring. The covalent nature (^1L_b) of the first excited state (Figure 4b) is indicated by the D_{ii} elements, which do not vary significantly from those found for the ground state (Figure 5b). The excitation is of benzene−benzene type, as shown by the general decrease of the P_{ij} elements (change of the spin coupling pattern) in the benzene ring, with an overall decrease of the bond order. The second excited state is the polar ^1L_a state (Figure 4c). The charge-transfer character can be seen from the occupation numbers (D_{ii} elements). Thus, the occupation of the nitrogen orbital is reduced to 1.40, and the charge is transferred to the C_4 and C_7 carbons (occupations 1.24 and 1.20, respectively). The bonding structure given in Figure 4c reflects the changes in the P_{ij} elements with respect to the ground state (Figure 5c). Thus, the P_{ij} of the pyrrole double bond decreases to 0.17, and the N_1-C_2 one increases from 0.10 (for S_0) to 0.33. In the benzene moiety, the value for C_5-C_6 increases from 0.27 (for S_0) to 0.36. Finally, the third excited state at the FC geometry is a biradical state (^1B_b, Figure 4d). The occupation numbers (D_{ii} elements) show no significant charge transfer (Figure 5d), while the bond orders (P_{ij} values) in the pyrrole ring decrease, leaving an uncoupled electron in C_2. This is an indication of the biradical nature of this state.

Valence-bond analyses were also carried out for the optimized structures near the FC geometry (**S_1-Min** and **S_1-Exc**). The resonance structures derived at these geometries are the same as those obtained at the FC geometry. To verify the correlation diagram of Figure 3b, the valence-bond analysis was also carried out for the S_3 state (biradical) of **S_1-Exc**. The computed D_{ii} and P_{ij} elements are given in Figure 5e. At this geometry, the valence-bond structure for the biradical state (Figure 3b) is in resonance with the ^1B_b state at the Franck−Condon geometry, and this proves that the biradical state that participates in the hydrogen transfer has its origin in the spectroscopic ^1B_b state of TRP.

The valence-bond formulas for the degenerate states at the intersection **CI-S_1/S_0** are shown in Figure 3b on structures **S_1-Taut** and **S_0-Taut**. The two structures are related by an intramolecular electron transfer from the side chain to the chromophore. This is clear from the occupation numbers of the side-chain orbitals, which are 1.97 and 1.03 for **S_0-Taut** and **S_1-Taut**, respectively (Figure 5f and g). From the P_{ij} elements (obtained localizing only the eight active orbitals of the chromophore), the chromophore for **S_0-Taut** has a closed-shell structure. In contrast to this, **S_1-Taut** has a delocalized radical on the benzene moiety of the chromophore.

Vertical Excitation Energies and Excited-State Complex Formation. The experimental UV-absorption spectrum of TRP

(17) Frisch, M. J.; Trucks, G. W.; Schlegel, H. B.; Gill, P. M. W.; Johnson, B. G.; Robb, M. A.; Cheeseman, J. R.; Keith, T.; Petersson, G. A.; Montgomery, J. A.; Raghavachari, K.; Al-Laham, M. A.; Zakrzewski, V. G.; Ortiz, J. V.; Foresman, J. B.; Cioslowski, J.; Stefanov, B. B.; Nanayakkara, A.; Challacombe, M.; Peng, C. Y.; Ayala, P. Y.; Chen, W.; Wong, M. W.; Andres, J. L.; Replogle, E. S.; Gomperts, R.; Martin, R. L.; Fox, D. J.; Binkley, J. S.; Defrees, D. J.; Baker, J.; Stewart, J. P.; Head-Gordon, M.; Gonzalez, C.; Pople, J. A. *Gaussian 99*, revision C.1; Gaussian, Inc.: Pittsburgh, PA, 1999.
(18) González, D. Ph.D. Thesis, University of London, 2001.
(19) (a) Deumal, M.; Novoa, J. J.; Bearpark, M. J.; Celani, P.; Olivucci, M.; Robb, M. A. *J. Phys. Chem. A* **1998**, *102*, 8404−8412. (b) Garavelli, M.; Celani, P.; Bernardi, F.; Robb, M. A.; Olivucci, M. *J. Am. Chem. Soc.* **1997**, *119*, 6891−6901. (c) Bernardi, F.; Celani, M.; Olivucci, M.; Robb, M. A.; Suzzi-Valli, G. *J. Am. Chem. Soc.* **1995**, *117*, 10531−10536.

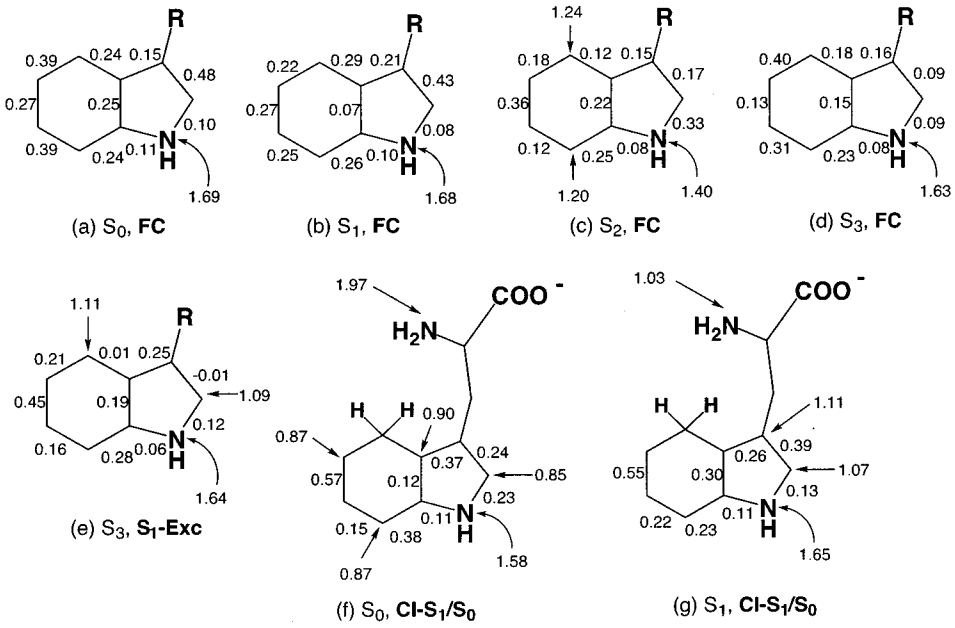

Figure 5. Valence-bond analysis for relevant states and structures: P_{ij} elements (for bond order) and selected D_{ii} elements (for occupations of localized orbitals, shown by arrows).

Table 1. Vertical Energies for TRP (in eV)

	vertical		0–0 transitions		
state	CAS	CAS-MP2	CAS	CAS-MP2	expt
S_1 (^1L_b)	4.98	5.16	4.63	4.93	4.32[a]
S_2 (^1L_a)	6.19	6.15			4.6−4.7[b]
S_3 (^1B_b)	6.34				5.58[c]

[a] 0−0 transition from jet-cooled experiments. [b] Estimated vertical excitation. [c] 3-Methylindole.

in the gas phase shows overlap of the ^1L_b and ^1L_a states.[4] The origin of the ^1L_b band could be identified around 286 nm (4.32 eV), where six close-lying bands were assigned as corresponding to the 0−0 transitions of six different side-chain conformers.[20] Although the origin of the ^1L_a band has not been determined experimentally, a value of 4.7 eV for the vertical excitation can be estimated if the two states are assumed to be as close as in indole (0.4 eV difference).[21] Our calculated CASSCF(10,9)/6-31G* vertical excitation values are 4.98 and 6.19 eV for the ^1L_b and the ^1L_a states, respectively, while the 0−0 excitations are 4.63 and 5.46 eV (see Table 1). The calculated vertical excitation for the third excited state (^1B_b) is 6.34 eV (experimental value 5.58 eV for 3-methylindole[22] and 5.80−6.02 eV for indole[23]). The resonance structures that describe the ground state and the three lowest excited states, obtained with the help of a valence-bond type analysis, are shown in Figure 4. The first excited state is a benzene−benzene type excitation, while S_2 and S_3 are ionic and biradical structures, respectively. Thus, our CASSCF calculations reproduce the three lowest excited valence states of TRP in the correct order at the FC geometry. However, the vertical energy of the ^1L_a state is overestimated with respect to the ^1L_b state by 0.7−0.8 eV (16−18 kcal mol^{-1}). This deviation from experiment is similar to the one obtained by Serrano and Roos in a comparable CASSCF calculation for indole.[23] In our case, inclusion of the MP2 correlation energy did not correct this deviation (see Table 1). In fact, it is known that to reproduce the experimental values accurately, an improved CASSCF description of the wave function (by adding Rydberg-type orbitals[23] or doubling the active space[18]) is necessary together with the MP2 correction. Rather than reproducing the experimental vertical energies, we were interested in the hydrogen-transfer process, and therefore we did not follow this procedure.

Near the Franck−Condon (FC) geometry, we optimized two structures for the lowest excited state (Figure 4). These are **S_1-Min**, the minimum of the covalent ^1L_b state, and **S_1-Exc**, a minimum of ^1L_a ionic wave function. The bond lengths shown in Figure 4 are the most significant values at the FC geometry, at **S_1-Min**, and at **S_1-Exc**. At **S_1-Min**, the main geometric changes with respect to the FC minimum are a lengthening of the bonds of the benzene moiety, which is in accordance with the description of the state as benzene−benzene excitation. In contrast to this, the main changes of the ring bond lengths in **S_1-Exc** are a shortening of N_1-C_2 and C_5-C_6 and a lengthening of C_2-C_3. However, the most significant feature of **S_1-Exc** is the formation of a weak hydrogen bond between an ammonium proton and the C_4 atom. Thus, the $H-C_4$ distance is reduced from 2.69 Å at the FC geometry to 2.09 Å at **S_1-Exc**. From the point of view of the energetics, the intramolecular excited-state complex **S_1-Exc** is a shallow minimum on the surface of S_1 and lies 3.1 kcal mol^{-1} above **S_1-Min** at the CAS-MP2 level (see Figure 1). The TS between **S_1-Min** and **S_1-Exc** was located using partial numerical derivation of the corresponding internal coordinate (the C−H distance of the hydrogen bond). The optimized structure, **S_1-TS$_1$**, lies very close to **S_1-Exc** (C_4-H distance 2.11 Å), and the activation barrier from **S_1-Min** is 3.2 kcal mol^{-1}. The analytical frequency calculation for **S_1-TS$_1$** with a reduced active space gave no imaginary frequency, but instead three lowest positive frequencies below 100 cm^{-1}. This reveals the flat nature of the potential energy surface in that region.

(20) Rizzo, T. R.; Park, Y. D.; Peteanu, L. A.; Levy, H. D. *J. Chem. Phys.* **1986**, *84*, 2534−2541.
(21) Fender, B. J.; Sammeth, D. M.; Callis, P. R. *Chem. Phys. Lett.* **1995**, *239*, 31−37.
(22) Albinsson, B.; Nordén, B. *J. Phys. Chem.* **1992**, *96*, 6204−6212.
(23) Serrano-Andrés, L.; Roos, B. O. *J. Am. Chem. Soc.* **1996**, *118*, 185−195.

The interconversion of the ^1L_a and ^1L_b states occurs along an avoided crossing path associated with a conical intersection between S_1 and S_2. Such an intersection was optimized. However, we expect that the computed topology will be affected by our overestimating the energy of the ^1L_a state relative to the ^1L_b one, and the details of the crossing topology will not be discussed further. Moreover, our error computing the energies of the ionic state implies that the energy barrier for the formation of the ionic structure **S_1-Exc** from the covalent one **S_1-Min** is probably lower than our calculated value of 3.2 kcal mol^{-1}. In principle, the formation of our calculated excited-state complex **S_1-Exc** is in agreement with the observation of a broad red shift in a highly resolved jet-cooled study of TRP fluorescence, upon excitation of the ^1L_b absorption of one of the six conformers.[20] This is an experimental indication of fast formation of an excited-state complex, and it agrees with our results. However, the gas-phase experiment is not really comparable to our calculation, because gas-phase TRP is in its neutral form, and our calculations model the zwitterionic isomer.

In summary, our results near the Franck−Condon region have to be treated with caution because of the poor reproduction of the ionic state. This is due, at least in part, to contaminating Rydberg states. However, this effect should disappear with the formation of the hydrogen bond to the chromophore, because the charge density in the chromophore is reduced, and the energy of the Rydberg states will rise. Therefore, we conclude that our results for the hydrogen-transfer process will be reliable.

Characterization of CI-S_1/S_0. For the calculation of the hydrogen-transfer transition structure at the geometry of **S_1-TS-H**, the active space was extended to (12,11) by inclusion of the σ(N−H) and σ*(N−H) orbitals. An intrinsic reaction coordinate (IRC) from **S_1-TS-H** in the direction of forward hydrogen transfer was carried out with the full active space (12,-11), using the force constants calculated with a reduced (8,8) active space. The IRC was interrupted at a point of near degeneracy between the excited and the ground state, where the optimization fails to converge. At this point, the σ and σ* orbitals of the newly formed carbon−hydrogen bond were removed from the active space (occupations close to 2 and 0, respectively). Optimization of the intersection with a (10,9) active space led to **CI-S_1/S_0**. With this active space, the intersection was optimized using an approximation where the coupled MCSCF equations were not solved.[24] To characterize the intersection in detail, the π orbital with highest occupation was removed from the active space, and the intersection was reoptimized with the remaining (8,8) active space solving the coupled MCSCF equations. At this level of theory, no stationary minimum could be optimized in the excited state. The initial parts of the two ground-state paths given in Figure 1 were optimized with IRC calculations (2.60 au in the direction of **S_0-Taut** and 1.1 au in the direction of **S_0-Degr**). The initial relaxation direction (IRD) was computed with an algorithm described previously and provided the starting points for the IRC calculations.[25] These calculations rigorously characterize the intersection as peaked, using the terminology of Ruedenberg.[26] The ground-state tautomer **S_0-Taut** was optimized at the HF/6-31G* level, and the decarboxylated pair **S_0-Degr** shown in Figure 1 was optimized at the B3LYP/6-31G* level. The geometry optimization of **S_0-Degr** proves that ground-state decarboxylation from the intersection **CI-S_1/S_0** is barrierless. The energies of **S_0-Taut** and **S_0-Degr** were recalculated at the CASSCF(10,9)/6-31G* level, using state-averaged orbitals (values given in Figure 1).

To assess the effect of solvation on our computed topology, and to exclude the possibility that the calculated decarboxylation path may be an artifact of incorrect treatment of the negative charge of the carboxylate, we repeated the optimization of **CI-S_1/S_0** adding a water molecule to the system. The water molecule was loosely bound to the carboxylate function by a hydrogen bridge. The reoptimization of the S_0/S_1 intersection at the CASSCF(10,9)/6-31G* level for the TRP−water complex gave essentially the same result as for the TRP molecule, the only difference being that the carbon−carbon bond was more stretched in the dimer (1.84 Å). This is due to stabilization of the closed-shell (ionic) state of the tautomer by the water molecule, which induces a displacement of the intersection along the bond cleavage coordinate. The investigation of the dimer was not carried further, but this calculation shows that the computed decarboxylation path is correct and does not disappear upon inclusion of the solvent.

Discussion of the Reaction Mechanism. Our calculations on the TRP potential energy surface near the FC region show that the first step in the hydrogen-transfer-induced fluorescence quenching is the formation of an ionic (^1L_a) excited-state complex, **S_1-Exc**, on the S_1 surface (see Figure 1 and Results section). The key feature of the S_1/S_2 crossing region is the change of wave function character from covalent to ionic. Therefore, after excitation, **S_1-Exc** can be accessed from the ^1L_b state via the low-barrier-avoided crossing, or from the ^1L_a state via decay through an intersection between S_1 and S_2. In **S_1-Exc**, the molecule is prearranged for the transfer of the H-bonded proton to the C_4 carbon of the benzene moiety, where negative charge density gets accumulated (see Figure 4). A proton-transfer transition structure, **S_1-TS-H**, was optimized on the surface of S_1 (see Figure 1). An analytical frequency calculation with a slightly reduced (8,8) active space gave a single imaginary frequency, and an IRC calculation from **S_1-TS-H** in the direction opposite to the proton transfer led to **S_1-Exc**. The activation energy starting from **S_1-Exc** was 0.8 kcal mol^{-1} at the CAS-MP2 level.

The proton-transfer coordinate, in the direction that transfers the hydrogen to the chromophore, is highly exothermic. Crucially, the mechanism switches from proton to hydrogen radical transfer along the reaction coordinate. The resulting coupled proton and electron transfer can be rationalized with the correlation diagram outlined in Figure 3b. The correlated excited states are the ionic (^1L_a) and the biradical (^1B_b) states (the ^1L_b state, which is S_2 at **S_1-Exc**, has been left out because it plays no role during the hydrogen transfer). Along the calculated reaction coordinate of S_1, represented by a full line, the process starts as a proton transfer, because the wave function of S_1 is purely ionic at the geometries of **S_1-Exc** and **S_1-TS-H**. However, as the reaction progresses beyond the TS, single-point calculations show that the mixing between the ionic and the

(24) (a) Bearpark, M. J.; Robb, M. A.; Schlegel, H. B. *Chem. Phys. Lett.*. **1994**, *223*, 269−274. (b) Ragazos, I. N.; Robb, M. A.; Bernardi, F.; Olivucci, M. *Chem. Phys. Lett.* **1992**, *197*, 217−223.

(25) Garavelli, M.; Celani, P.; Fato, M.; Bearpark, M. J.; Smith, B. R.; Olivucci, M.; Robb, M. A. *J. Phys. Chem. A* **1997**, *101*, 2023−2032.

(26) Atchity, G. J.; Xantheas, S. S.; Ruedenberg, K. *J. Chem. Phys.* **1991**, *95*, 1862−1876.

Scheme 3

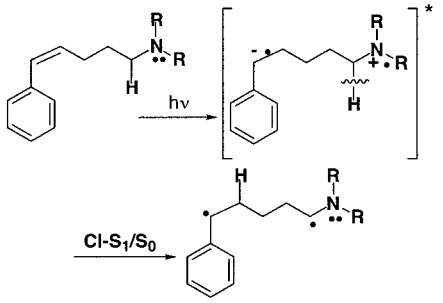

biradical states sets in and induces a change in the character of the wave function. Thus, the reaction ends in the charge-transfer structure that correlates with the ^1B_b state. The result is a net hydrogen radical transfer. Exploratory calculations suggest that the mixing of the ^1L_a and ^1B_b states on the reaction coordinate might occur along a truly avoided crossing, because no conical intersection between the two states could be located. The surface crossing would provide an efficient reaction path from the spectroscopic S_3 state (^1B_b), but the existence of such a path seems questionable. In any case, the mechanism of sequential proton and electron transfer described here is similar to the one found on the ground state of the azoalkane and dichloromethane model system.[3a,b] However, in the azoalkane case, the coupling is weak, and the crossing is weakly avoided. In the present case, the coupling between the two states is strong, and the crossing is strongly avoided, and the wave function changes character smoothly along the reaction coordinate.

The hydrogen transfer leads directly to the conical intersection **CI-S_1/S_0** (see Results section), which lies approximately 31.6 kcal mol^{-1} below **S_1-Exc**. The two degenerate states are shown in Figure 3b. They are the closed-shell ground-state tautomer and a biradical generated by a formal charge transfer between the side-chain nitrogen and the indole moiety. In fact, the charge transfer comes from a delocalized side-chain orbital (see Results section). This provides stabilization by delocalization of the transferred charge. In turn, the delocalization of the charge along the carbon−carbon σ bond accounts for its large distance (1.74 Å at **CI-S_1/S_0**) and induces the cleavage of the bond. The photodecarboxylation described here can be generalized as the cleavage of a bond in α position of an amine, after photochemical generation of the amine radical cation. This reaction has been also described for styrenes with an amino substituted side chain (Scheme 3).[27] In these systems, the amine radical cation is generated by photochemically induced electron transfer to a styrene moiety, and the cleavage of the adjacent carbon hydrogen bond is assisted by the styrene anion. The reaction results in a biradical which subsequently cyclizes, and according to the mechanism elucidated for TRP, the decay of the excited molecule to the ground state should take place during the cleavage of the carbon hydrogen bond.

The two ground-state decay routes from **CI-S_1/S_0** (determined with IRC calculations, see Results section) follow the gradients of the crossing states, which correspond roughly to the carbon−carbon bond stretching coordinate. This coordinate is also the gradient difference at the intersection, one of the two degeneracy-lifting coordinates[1] along which the decay will occur. Following the bond stretching in the elongation direction, a barrierless decay path leads from **CI-S_1/S_0** to complete decarboxylation. The degradation product **S_0-Degr** is a biradical (Figures 1 and 3b), and intramolecular hydrogen transfer should lead to tryptamine, which has been identified experimentally as one of the products of TRP photolysis.[4,11a] In the opposite direction of the bond stretch, shortening of the bond leads along a barrierless path to the ground-state tautomer **S_0-Taut**, precursor of the deuterated product observed when the photolysis is carried out in a deuterated solvent.[10] In principle, the ratio between the two photoproducts **S_0-Taut** and **S_0-Degr** could be estimated comparing the gradients of the crossing states along the calculated decay paths.[26] Our calculations would predict a similar phototautomerization and photodecarboxylation ratio, since the slopes of both decay paths are similar. However, the experimental data show that the quantum yield for phototautomerization, determined in a deuterium incorporation experiment, is substantially higher (0.14)[10b] than the quantum yield for decarboxylation (0.008).[11a] Thus, it is clear that the level of accuracy of our calculations is not high enough to allow for a quantitative estimation of the reaction outcome, because our computations do not include the correlation energy along the decarboxylation path and do not consider the dynamics of the reaction. In any case, the two ground-state intermediates **S_0-Taut** and **S_0-Degr** are plausible candidates for the intermediate (τ = 44 ns) detected by absorption measurements in early experiments of TRP photolysis in water by Brent and Hayon, which was originally assigned as a triplet (T_1 in the cited reference).[9g]

The key role of the charge transfer in the decay is evidenced by calculations where the side-chain donor orbital was removed from the active space. This is equivalent to eliminating the ^1B_b state in the correlation diagram of Figure 3b. In this "artificial" situation, with a reduced (8,8) active space, the excited-state tautomer **S_1-Taut** would be a minimum on the potential energy surface, and the radiationless decay would take place at a sloped conical intersection with a substantial barrier (13.0 kcal mol^{-1} at the CAS-MP2 level), associated with a distortion of the benzene moiety.[28] This provides evidence that the proton-transfer alone does not account for the low-barrier deactivation channel and emphasizes the role of the side chain in enabling the charge transfer coupled to the protonation. However, the ring distortion process may account for the radiationless decay induced by H_3O^+ in donor-substituted naphthalenes, where the hydrogen transfer and decarboxylation mechanism is not possible.[15b] Furthermore, our calculations clarify the selectivity of the proton-induced quenching of aromatic compounds observed experimentally in the group of Shizuka.[15] The intramolecular fluorescence quenching takes place in phenyl- and naphthylalkylamines[15a,c] and is explained by our calculated coupled proton- and charge-transfer mechanism, followed presumably by cleavage of a side-chain bond. In turn, this mechanism is not possible for the parent indole[4] and naphthalene systems,[15a] which explains the absence of H_3O^+-induced quenching there.

Conclusions

Hydrogen transfer alone is not sufficient to induce the intramolecular quenching of TRP fluorescence, and of singlet

(27) Lewis, F. D.; Reddy, G. D.; Bassani, D.; Schneider, S.; Gahr, M. *J. Am. Chem. Soc.* **1994**, *116*, 597−605.

(28) The degeneracy in this case is induced by an out-of-plane bending of the C_5 aromatic carbon (a kink in the benzene ring, see Cartesian coordinates in Supporting Information).

π,π^* excited states, in general. According to a model based on correlated states, fluorescence quenching along a hydrogen-transfer coordinate can, in general, only take place when the ground and the excited states of the reactant are hydrogen acceptors. This is the case for n,π^* excited states, as seen previously for an azoalkane model.[3a,b] However, in the π,π^* case (TRP), the ground state is not a hydrogen acceptor, and the excited hydrogen transfer is adiabatic. The process is a coupled proton and electron transfer and has its electronic origin in the interaction between two excited states (ionic and biradical). Thus, the hydrogen transfer leads to an excited-state tautomer, and the radiationless decay to the ground state takes place along an additional, barrierless decarboxylation coordinate. The intersection acts as a bifurcation, and the transition state for the excited-state hydrogen transfer serves two products: the ground state tautomer and a decarboxylated photodegradation product, precursor of tryptamine. In summary, together with previous results for an azoalkane and dichloromethane model system, our results for the fluorescence quenching of zwitterionic TRP show that the quenchers act not only as hydrogen donors. On the contrary, they are involved in other steps of the quenching, such as electron transfer between the quencher and the chromophore and, in the TRP case, decarboxylation of the amino acid side chain.

Acknowledgment. All computations were carried out on an IBM-SP2 funded jointly by IBM-UK and HEFCE (U.K.). We are grateful to the European Community for a Marie Curie Fellowship to L.B. (Grant No. ERB4001GT964926). The collaboration between M.A.R. and M.O. is financed by a Nato Grant CRG 950748.

Supporting Information Available: Absolute and relative energies (Table S1); spin-exchange density matrix elements and diagonal elements of the one-electron density matrix (Table S2); and Cartesian coordinates of reported structures (PDF). This material is available free of charge via the Internet at http://pubs.acs.org.

JA016915A